Available online at www.sciencedirect.com

ScienceDirect

journal homepage: www.elsevier.com/locate/issn/15375110

Research Paper

Uncertainty in the measurement of indoor temperature and humidity in naturally ventilated dairy buildings as influenced by measurement technique and data variability

Sabrina Hempel [a,*], Marcel König [a], Christoph Menz [b], David Janke [a], Barbara Amon [a], Thomas M. Banhazi [c], Fernando Estellés [d], Thomas Amon [a,e]

[a] Leibniz-Institute for Agricultural Engineering and Bioeconomy (ATB), Max-Eyth-Allee 100, 14469 Potsdam, Germany
[b] Potsdam Institute for Climate Impact Research (PIK), P.O. Box 60 12 03, 14412 Potsdam, Germany
[c] University of Southern Queensland, Toowoomba, Queensland, Australia
[d] Institute of Animal Science and Technology, Universitat Politecnica de Valencia, Camino de Vera S/n, 46022, Valencia, Spain
[e] Department Veterinary Medicine, Free University Berlin, Robert-von-Ostertag-Str. 7-13, 14163 Berlin, Germany

ARTICLE INFO

Article history:
Received 25 November 2016
Received in revised form
25 October 2017
Accepted 8 November 2017
Published online 29 November 2017

Keywords:
Microclimatic variability
Measurement uncertainty
Heat stress

The microclimatic conditions in dairy buildings affect animal welfare and gaseous emissions. Measurements are highly variable due to the inhomogeneous distribution of heat and humidity sources (related to farm management) and the turbulent inflow (associated with meteorologic boundary conditions). The selection of the measurement strategy (number and position of the sensors) and the analysis methodology adds to the uncertainty of the applied measurement technique.

To assess the suitability of different sensor positions, in situations where monitoring in the direct vicinity of the animals is not possible, we collected long-term data in two naturally ventilated dairy barns in Germany between March 2015 and April 2016 (horizontal and vertical profiles with 10 to 5 min temporal resolution). Uncertainties related to the measurement setup were assessed by comparing the device outputs under lab conditions after the on-farm experiments.

We found out that the uncertainty in measurements of relative humidity is of particular importance when assessing heat stress risk and resulting economic losses in terms of temperature-humidity index. Measurements at a height of approximately 3 m–3.5 m turned out to be a good approximation for the microclimatic conditions in the animal occupied zone (including the air volume close to the emission active zone). However, further investigation along this cross-section is required to reduce uncertainties related to

* Corresponding author.
https://doi.org/10.1016/j.biosystemseng.2017.11.004

the inhomogeneous distribution of humidity. In addition, a regular sound cleaning (and if possible recalibration after few months) of the measurement devices is crucial to reduce the instrumentation uncertainty in long-term monitoring of relative humidity in dairy barns.

Nomenclature

NVB	naturally ventilated barn
THI	temperature-humidity index
T	temperature, °C
H	relative humidity, %
t	time (dependent on the content in seconds or in days)
ρ_τ	autocorrelation for lag τ
τ	time lag
E	expected value operator
σ	variance of time series
x	time series
$\bar{x}$	mean value of the time series
N	length of the time series
P	power spectral density
f	frequency
n_q	Nyquist frequency
ΔT	sampling interval
U	uncertainty
i, j, k	indices for uncertainty estimation indicating time point, sensor and random number
r	realisation of the random process
DT	Dummerstorf
GK	Gross Kreutz
NGT	night from 10 pm to 4 am
MRNG	morning from 4 am to 10 am
NOON	noon from 10 am to 4 pm
EVE	evening from 4 pm to 10 pm

1. Introduction

Animal husbandry must be animal- and environment-friendly to be socially acceptable and sustainable. The ventilation of livestock houses is a key driver for animal welfare and pollutant emissions. It is crucial to remove pollutants, excess moisture and heat from livestock houses. Two principal options exist; the application of mechanical and natural ventilation systems.

In Europe, the economically highly relevant dairy cattle sector is predominantly characterised by intensive milk production with high-yielding cows in naturally ventilated barns (NVB) (Algers et al., 2009). The main advantage of these buildings is their energy saving property since in general natural ventilation does not require electrical energy to operate fans. However, this housing system is particularly vulnerable to climate change as the microclimate in the barn directly depends on the ambient climatic conditions.

Larger variability and more extreme conditions in the regional climate are projected under various climate change scenarios (Christensen et al., 2007). That might affect animal welfare as well as gaseous emissions. In addition, there is an indirect impact of climate change on the net production associated with the farms as, for example, an increase in management related expenses and a decrease in reproduction rate and milk yield is expected under heat stress conditions (Kuczynski et al., 2011). However, the quantification of these impacts is challenging, as the relations between the impacts and the microclimatic conditions are complex and only partly described by the documented empirical equations. Moreover, uncertainty in the monitoring of the related microclimatic key parameters (temperature, humidity and local air velocity) will increase uncertainties in the impact assessment.

Classically, heat stress is assessed by a temperature-humidity index (THI) which is based on point measurements of air temperature and relative humidity (NRC, 1971; Armstrong, 1994; Kendall et al., 2006). Sometimes additional variables are taken into account that can increase or decrease the heat load such as radiation or air speed (Mader, Davis, & Brown-Brandl, 2006). The THI increase is associated with decreases in dry matter intake, milk yield and milk quality as well as an increase in water consumption (Bohmanova, Misztal, & Cole, 2007; Bouraoui, Lahmar, Majdoub, Djemali, & Belyea, 2002; Carabano et al., 2016). It is also documented in literature that rising THI values result in a reduction in milk fat and protein content (Ravagnolo, Misztal, & Hoogenboom, 2000). These impacts can be translated into economical losses on the farm.

Moreover, the microclimatic conditions in a barn affect the emissions that are attributed to the barn, as outlined hereafter.

Ammonia release from the floor of cattle houses, for example, is strongly affected by air and manure temperature and by air velocity and turbulence intensity above the ammonia releasing surface (Bjerg et al., 2013; Rong, Liu, Pedersen, & Zhang, 2014; Saha et al., 2014; Schrade et al., 2012). In addition, there is a relation between relative humidity of the barn air and ammonia emissions from naturally ventilated dairy barns (Saha et al., 2014). The relative humidity of the air surrounding the manure influences the humidity in the manure with low values speeding up evaporation and higher values slowing it down. The humidity in the manure, on the other hand, changes the pH level, which is again a crucial parameter for the estimation of ammonia release rates (Bjerg et al., 2013).

In the case of greenhouse gas emissions, the release may occur from manure and from the gastrointestinal tract. In the case of dairy farming, greenhouse gas emissions (particularly methane emissions) are mainly related to the cows rumen metabolism (Monteny, Bannink, & Chadwick, 2006). It had been shown that methane emissions are associated with the average air temperature and relative humidity in the barn (Saha et al., 2014). The lowest methane emissions were documented when the cows were in the thermo-neutral zone (Hempel et al., 2016). In this sense, the emission rate is also related to the THI attributed to the barn.

It is state of the art either to use outdoor temperature and humidity values or to consider daily averages or maxima measured in the centre of the building to estimate the THI. However, these microclimatic parameters are not homogeneously distributed in the barn as neither the heat and humidity sources nor the air velocity are uniform throughout the barn (Hempel et al., 2015). To monitor the microclimatic conditions more efficiently, it is necessary to identify monitoring locations that provide an accurate and representative assessment for the entire livestock building or particular crucial zones (e.g., the emission active zone or the animal occupied zone) and to estimate the total uncertainty attributed to these measurements (Banhazi, 2013).

Currently there are no readily available recommendations for the number and positioning of measurement devices or sampling frequencies to achieve a particular degree of accuracy in the measurements of microclimatic conditions.

The first aim of this study is to investigate the suitability of selected reference points and sampling intervals. In this context, the representativeness of points and intervals means that the selected sample should at least better than all other tested measurement configurations capture the range of variability in the measured quantity in order to lead to suitable management decisions for animal welfare. We want to evaluate the representativeness of different measurement positions above the animals in order to provide a reference for on-farm monitoring in commercial barns where measurements close to the animals might be too effortful. Hence, we analysed data from spatially distributed sensors in two barns for deviations from the spatial mean at each time as well as the persistence and periodicity in the spatially averaged time series of the barn climate variables during hot and cold periods. The second aim is to quantify different sources of uncertainty in the measurements of microclimatic conditions in naturally ventilated barns. Uncertainties related to the measurement setup and the selection of measurement locations are evaluated and discussed in detail with regard to heat stress and production loss.

2. Material and methods

Our study is based on data sets from three locations: long-term measurements at two farms in Germany and lab experiments conducted at the Leibniz-Institute for Agricultural Engineering and Bioeconomy. The data collection and data analysis is described in detail in this section.

2.1. Data collection

2.1.1. On-farm experiment barn "Dummerstorf"

The first on-farm data set was based on long-term measurements carried out at a commercial naturally ventilated dairy building, located in Mecklenburg-Vorpommern, north-east Germany (approximately 217 km north-west of Berlin, coordinates: 12.2291666 E, 54.0125 N, 42 m above sea level). The dairy building is 96.15 m long and 34.20 m wide. The height of the sheet metal roof varies from 4.2 m at the sides to 10.7 m at the gable peak. The internal room volume of the barn is 25,499 m^3 (70 m^3 per animal), and was designed for 364 dairy cows (loose housing with littered lying cubicles and concrete walking alleys that were regularly scraped). The building has an open ridge slot (0.5 m), space boards (115 mm width and 22 mm thickness of wood board having solid core and spaced by 25 mm) in the gable wall of the western end of the building and a sheet metal wall at the eastern end. There is one gate (4 m × 4.4 m) and 4 doors with adjustable curtains (where two doors are 3.2 m × 3 m, and two doors are 3.2 m × 4 m) in each gable wall. The long sidewalls are protected by nets and air is introduced via adjustable curtains (Hempel et al., 2016).

Temperature and relative air humidity were logged every 10 min (instantaneous value for the second) using Comark Diligence EV N2003 sensors (Comark Limited, Hertfordshire, UK; temperature accuracy of ±0.5 °C for −25 °C to +50 °C, and relative humidity accuracy of ±3% for −20 °C to +60 °C, 0%–97% relative humidity non condensing).

We used data from an existing setup, where sensors were placed along two lines in a height of 3.3 m. Some of the sensors of the setup could not be taken into account due to an insufficient available amount of data. This resulted in four sensor positions with a distance of approximately 20 m between the sensors and to the walls. This measurement setup is depicted in Fig. 1.

The two sensors at the northern and the southern corner of the barn were excluded in this study as the available amount of data was insufficient. This resulted in four sensor positions with an distance of approximately 20 m between the sensors. The data used in this study were collected during 24-03-2015 and 27-11-2015.

2.1.2. On-farm experiment barn "Gross Kreutz"

The second on-farm data set is based on long-term measurements carried out at a naturally ventilated dairy building for education and research, located in Brandenburg, Eastern Germany (approximately 56 km west of Berlin, coordinates: 12.7791666 E, 52.4041666 N, 32 m above sea level) The dairy building is 38.88 m long, 17.65 m wide. The height of the fibre cement roof varies from 6.2 m at the gable peak to about 3.6 m at the sides. The roof is asymmetric where the gable peak is located approximately 7 m away from the feeding alley (cf. Fig. 2, for example, the middle between sensor E and R). Two window arrays are included in the roof. The internal room volume of the barn is 4,529 m^3 (90 m^3 per animal). The barn is designed for 50 dairy cows in loose housing with littered lying cubicles. Most of the walking alleys are equipped with a concrete floor that was scraped once per hour; a small

Fig. 1 – Description of the measurement site Dummerstorf: Layout of the barn (north front at the top of the map) and sensor positions (left), photography of the barn viewed from the main prevailing wind direction (middle, source: ATB) and a map of the farm indicating the position and orientation of the barn (right, source: Homepage Gut Dummerstorf).

Fig. 2 – Description of the measurement site Gross Kreutz: Layout of the barn (north front at the bottom of the map) and sensor positions (left), photography of the barn viewed from the main prevailing wind direction (middle, source: ATB) and a map of the farm indicating the position and orientation of the barn (right, source: Google maps).

area at the end of the scraper (in front of the automated milking system) is equipped with slatted floor. At the southern gable wall the opening size is reduced by several components embedded in the main building (cf. Fig. 2): A porch (3.55 m × 4.1 m floor size) with a cesspool at the western end, a room for the milking robot (fully closed with 9 m × 4.1 m floor size) in the middle, and a calf house (5.1 m × 14.4 m floor size) at the eastern side. The northern gable wall has two large gates. The western end of the building is open up to about 1.5 m height while the eastern end is open up to the roof.

Temperature and relative air humidity were logged every 5 min (instantaneous value, shortest logging rate 10 s) using EasyLog USB 2+ sensors (Lascar Electronics Inc., USA; temperature accuracy of ±1 °C for −35 °C to +80 °C, and relative humidity accuracy of ±3.5% for −20 °C to +80 °C, 0%–100% relative humidity).

In contrast to the experiment in Dummerstorf, here a new measurement setup with higher spatial resolution was designed, taking into account the different barn designs with smaller opening area per cow in Gross Kreutz, which was expected to result in lower rates of air exchange and mixing. The sensors were positioned at eight locations inside the building 3.4 m above the floor (cf. Fig. 2). In addition, a vertical profile of temperature and relative humidity measured at sensor position E (close to the automated milking system) was analysed. Therefore, additional sensors were placed 4.0 m, 4.6 m, 5.2 m and 5.8 m above the floor. The data used in this study were collected during 02-06-2015 and 05-03-2016 for the horizontal profile and during 02-03-2016 and 05-04-2016 for the vertical profile.

2.1.3. *Lab experiment – Validation of the temperature and humidity ensemble measurements*

In order to estimate the measurement uncertainty of the ensembles of temperature-humidity sensors used in our on-farm experiments we analysed the output of the same devices under lab conditions – once with the four Comark Diligence EV N2003 sensors (Instrument ensemble 1, day 0–2) and

once with the twelve EasyLog USB 2+ sensors (Instrument ensemble 2, day 3–5). These experiments were conducted after the on-farm measurements to capture the total measurement uncertainty which includes the instrumentation uncertainty, the aging process of the individual devices and the ensemble uncertainty (e.g., initial potential offset between the devices and the different measurement history of the individual devices).

Instrument ensemble 1: We considered the devices used in Dummerstorf. All four Comark devices were put into an incubator with constant water vapour content for about two days. First, the temperature in the incubator was kept at room temperature (approximately 18 °C). After several hours the heating of the incubator was turned on for 2 h with a target temperature of 30 °C to test the sensitivity for different regimes of temperature and relative humidity and the response time of the devices for temperature changes. By that the measured temperature in the incubator increased up to 33 °C. Afterwards the heating was turned off again and within approximately 2 h the temperature returned to ambient temperature. The devices remained in the closed incubator for another one and a half day.

Instrument ensemble 2: The devices used in Gross Kreutz were considered. Since the volume in the incubator was limited, the twelve EasyLog devices were put into a cold storage cell with a target temperature of 7 °C and constant water vapour content. Due to the hysteresis of the thermostat the actual temperature in the cold storage cell varied between 6 °C and 7.5 °C during the experiment which lasted for about one and a half day. In order to test the sensitivity for different regimes of temperature and relative humidity and the response time of the devices for temperature changes, all devices were put into a closed room with approximately 23 °C for another half day.

2.1.4. *Reference climate data*

Impact assessments typically rely on observational or simulated climate data for the considered region, while local long-term measurements (more than 30 years) for a farm are rarely available. Thus, in our study we investigate the dynamics of the evolution of temperature and relative humidity in the barn over several months and compare the results to the average dynamics in the regional climate represented by observational data from the national weather service. Time series of daily averaged temperature and relative humidity were collected from four weather stations of the DWD (German weather service) – two as close as possible to each farm. For the location Dummerstorf the stations Gross Lüsewitz (≈10 km from the farm) and Rostock-Warnemünde (≈19 km from the farm) were selected as the most representative stations for the regional climate. For the location Gross Kreutz the stations Brandenburg-Görden (≈18 km from the farm) and Potsdam (≈19 km from the farm) were used. All climate time series covered the years 1950–2000. In addition, for individual stations and time intervals, recent data from the years 2000–2015 was also available. While for the estimation of the average seasonal conditions the whole available data set was used, the estimation of the autocorrelation function relies on the data of the year 2000.

2.2. *Data analysis*

2.2.1. *Uncertainty*

In order to estimate the measurement uncertainty of the ensemble of sensors we calculated the standard deviation from each set of devices for each time step during the measurements in the lab. We define our total measurement uncertainty as twice the maximal observed standard deviation 2σ. Assuming a Gaussian normal distribution this corresponds to the 95% confidence interval.

In order to estimate also the uncertainty that may result from different response times of the devices, we compared the estimated uncertainty values for two cases - one omitting regimes with fast temperature transitions and one considering the entire time series from the validation experiment.

2.2.2. *Determinism*

In order to evaluate the predictability of the microclimatic conditions in the barns we consider two deterministic components of the spatially averaged long-term time series namely the periodicity and the persistence.

The persistence refers to the tendency of a time series to retain similar values, i.e. if the temperature is low at time t there is a high probability that it is low at time $t+\tau$ as well, if the duration between the two time steps is short enough. In highly persistent time series this temporal scale is very long. An indication of persistence and an estimation of the related temporal scale are provided by the autocorrelation function (Eq. (1)).

$$\rho_\tau = \frac{E[(x_{t+\tau}-\overline{x})(x_t-\overline{x})]}{\sigma^2} := \frac{\sum_{t=max(1,-\tau)}^{min(N-\tau,N)}(x_{t+\tau}-\overline{x})(x_t-\overline{x})}{\sum_{t=1}^{N}(x_t-\overline{x})^2} \quad (1)$$

Here ρ_τ refers to the autocorrelation for lag τ, E is the expected value operator and σ is the variance of the time series x with mean $\overline{x}$ and length N.

Autocorrelation, also called lagged correlation, refers to the correlation of a time series with its own past and future values. The correlation coefficient for selected time lags is determined and summarizes the strength of the linear relationship between present and past or future values for the given lags. Positive autocorrelation can be considered a specific form of persistence. For our calculations we used the function '*acf*' in the statistical software *R* with the estimator defined in Eq. (1) to obtain the autocorrelation function (R Core Team, 2015; Venables & Ripley, 2013).

The second measure that we considered is the periodicity, which implies that a particular state is regularly recurrent (e.g., high temperatures occur around noon and low around midnight each day). If the time series is periodic, this will be reflected also in the autocorrelation. An automated identification of important frequencies in the autocorrelation function is, however, not straightforward. An alternative way to identify dominant frequencies in a signal is the periodogram. It permits to detect frequencies that are smaller than half of the sampling rate of the discrete signal (so-called Nyquist frequency), which corresponds in our data sets to cycles longer than ten (for the EasyLog devices) or 20 min (for Comark devices), respectively (Vlachos, Philip, & Castelli, 2005). The periodogram can be calculated by discrete Fourier

transformation and results from the squared length of each Fourier coefficient (cf. Eq. (2)).

$$P(f) = \frac{1}{2N \cdot n_q}\left|\sum_{t=0}^{N-1} x_t exp\left(-i\pi t\frac{f}{n_q}\right)^2\right| \quad (2)$$

Here P is the power spectral density at frequency f which is a measure of a signal's intensity in the frequency domain. The power spectral density is calculated for a signal x sampled at N different times, i.e. our discrete time series of length N. The samples are uniformly spaced by Δt, which is the time interval of sampling (in this study five or 10 min, respectively). The Nyquist frequency results from this sampling interval as $n_q = (2\Delta t)^{-1}$. We calculated the periodogram using the function '*periodogram*' from the *R*-package 'TSA' (Chan & Ripley, 2012). Although the periodogram is known to exhibit high spectral leakage (which refers to a generation of artificial frequency components due to the finiteness of the signal), it can provide indication for the most dominant frequencies at least for short and medium length periods (Vlachos et al., 2005).

We compared the power spectrum of each time series with the spectrum of Gaussian white noise (i.e. a random signal having equal intensity at all frequencies). Therefore, for each of the considered microclimatic time series one hundred surrogate time series (realisations of Gaussian white noise with same length, mean and standard deviation as the original time series) were calculated. The periodograms at each frequency were estimated and the fifth highest estimate out of the one hundred was selected for the reference spectrum (i.e., the 95% percentile for each individual frequency).

2.2.3. *Comfort assessment*

In order to evaluate the expected individual comfort or discomfort of a person or animal in a warm microclimate in the barn additional state variables of the indoor air besides air temperature must be taken into account. For example, cold air with high relative humidity appears colder than dry air of the same temperature, while hot and humid air appears particularly warm. For that reason, in the 1970's the United States National Weather Service developed an temperature-humidity index that assigns a signal numeric value to the ambient atmospheric conditions. This value represents an effective air temperature and has been used to measure cow comfort in terms of heat stress since the early 1990's. Different versions of the index exist which differ in the weights assigned for the effect of humidity.

In this study, we determined a temperature-humidity-index (THI) for each time step in the measurements using Eq. (3) to assess the potential impact on animal welfare that results from the distribution of air temperature (T) in °C and relative humidity (H) in % in the barn (NRC, 1971; Armstrong, 1994; Ravagnolo et al., 2000; Kendall et al., 2006).

$$THI = (1.8 \times T + 32) - ((0.55 - 0.0055 \times H) \times (1.8 \times T - 26)) \quad (3)$$

According to Armstrong (1994), this measure can be used to subdivide the microclimatic conditions into "comfort zone" (THI < 72), "mild stress" (73 ≤ THI ≤ 78), "danger" (79 ≤ THI ≤ 84) and "emergency" (THI ≥ 85) (Armstrong, 1994).

In order to assess the uncertainty in the potential impact we considered the range of minimal and maximal expected THI based on the measured horizontal profile and the total measurement uncertainty in temperature and humidity. The entire uncertainties in T and H are propagated to the THI using a special case of Monte Carlo methods.

First, we estimated for each time step i and sensor j distributions of the temperature T_{ijk} and of the relative humidity H_{ijk} with N_k random numbers (cf. Eq. (4) and (5)). For this purpose, for each sensor j the actually measured values T_{ij} and H_{ij} were assumed to be mean values of Gaussian distributions. The standard deviation of the Gaussian distribution was defined as half of the associated measurement uncertainty U as derived from the validation experiments in the lab.

$$T_{ijk} = \frac{2}{\sqrt{2\pi}U_T} exp\left(\frac{-2(x_k - T_{ij})^2}{U_T^2}\right) \quad (4)$$

$$H_{ijk} = \frac{2}{\sqrt{2\pi}U_H} exp\left(\frac{-2(x_k - H_{ij})^2}{U_H^2}\right) \quad (5)$$

In this way, surrogate measurements for each sensor j and time point i were generated as normally distributed random numbers. The amount N_k of these random numbers was chosen such that in total $N_j \cdot N_k = 800$ random numbers approximate the empirical distributions in the horizontal profile (i.e., for Dummerstorf $N_k = 200$ random numbers time $N_j = 4$ sensor positions and for Gross Kreutz $N_k = 100$ random numbers times $N_j = 8$ sensor positions).

From this resulting empirical distributions of temperature and relative humidity $r = 1\,000$ realisations of all possible 640,000 combinations of T_{jk} and H_{jk} are selected randomly to estimate an empirical distribution of the THI for a selected time step i. This distribution takes into account the uncertainties from the ensemble of measurement devices and from the spatial variability of the temperature and humidity in the animal occupied zone.

Finally, we evaluated the resulting THI distributions as follows:

(1) For each time step i we calculated different quantiles (0,0.25,0.5,0.75 and 1) of the estimated THI distribution in order to reduce the amount of data for the analysis but still capture higher moments (e.g., skewness) of the distribution, which does not necessarily needs to be a Gaussian distribution. For each time series of quantiles, we defined individual heat stress events as periods where all consecutive time steps showed a $THI \geq 72$. Once a THI value was below the critical value the event stops. We considered the time series of the quantiles to evaluate the risk of giving false alarms or missing events.

(2) For each event, we determined the duration (number of time steps × sampling rate). The histogram of the durations was calculated. In order to construct the histogram, the first step was to bin the range of values (i.e., divide the entire range of values into a series of intervals). Here, we have chosen bins of 1 h. The cumulated sum of counts in these bins was considered to evaluate the probability of events below/above a given duration.

(3) We selected time frames with n time steps representing individual months (e.g., June) or times of the day (e.g., night defined as times between 10 pm and 4 am). For those time frames we determined the probability of THI to be above the critical threshold of 72 as the frequency of values with $THI > 72$ among all $n \times r$ values in the associated THI distribution.

3. Results

3.1. *Lab experiment – Validation of the temperature and humidity ensemble measurements*

The data from the validation experiment indicated a good agreement between the devices for the temperature measurements, but larger deviations for relative humidity (cf. Fig. 3). Taking into account only periods with slow temperature changes (i.e., (<3 °C h^{-1}), implying slow changes in relative humidity as well) the Comark devices were attributed with 0.4 °C uncertainty and the EasyLog devices with 0.6 °C. This is basically the instrumentation uncertainty as indicated by the manufacturer. For periods with fast transitions (>10 °C h^{-1}) the measurement uncertainty increased to 1 °C for Comark and 3 °C for EasyLog. In this case besides the instrumentation uncertainty, also random effects and the uncertainty related to the response time of the devices must be taken into account.

In the case of relative humidity, deviations of 7% relative humidity for EasyLog (up to 11% relative humidity for fast transitions) and 26% relative humidity for Comark were observed which is considerable larger than the instrumentation uncertainty indicated by the manufacturer. The obtained values refer to the total measurement uncertainty depending on various factors. These factors include the instrumentation uncertainty, random effects, uncertainty related to the response time of the devices, uncertainty resulting from aging effects and the individual measurement history of the different devices.

We also observed a bias depending on the duration that the devices were used under on-farm conditions. The same type of devices in use for about 9 months showed on average approximately 2%–4% higher relative humidity values than the set of devices that was in use for only 1 month under on-farm conditions before the validation experiments started.

3.2. *On-farm experiment barn "Dummerstorf"*

The time series of the spatially averaged temperature in the barn reflected the annual cycle of the ambient conditions with indoor values up to 34 °C in summer and down to 1 °C in spring and autumn as shown in Fig. 4. The observed distribution of temperature values during the year was almost symmetric with a mean of 15.0 °C and a median of 14.8 °C.

The distribution of the measured values of relative humidity on the other hand was very asymmetric with a mean of 82.7% and a median of 88.0%. One quarter of all values was above 95% relative humidity, about half of the values were above 85% relative humidity and three quarters were still above 70% relative humidity. The lowest values were measured in early May and late August with about 37% relative humidity. This corresponds with the annual cycle of relative humidity in the ambient climate where spring and summer are characterised by on average approximately 10% less relative humidity than autumn and winter (cf. Table 1).

In the case of temperature, even after 40 days there was a low but significant correlation between the signals of the original and the lagged time series. This indicates that the future values of the time series are to a certain degree (i.e. correlation coefficients $\geq$0.2) related to the past values over a period of about one month (cf. Fig. 4). In the case of relative humidity, no significant correlation was found anymore for a 10 days lag.

In the periodogram in Fig. 4, we found a strong peak at a frequency of 1 per day indicating the daily rhythm of the signal. Moreover, peaks occurred at 2 per day and 3 per day indicating an underlying subdaily rhythm which almost certainly is related to milking and cleaning activities which are conducted approximately every 8 h in this barn. In addition, several smaller peaks (highlighted by vertical lines in the Fig. 4) were found in the interval (0,1) which correspond to cycles on a weekly time scale: Around 0.4 per day, 0.45 per day and 0.55 per day both signals showed peaks which indicate periodicities around 2.5 and 2 days. Another peak occurred around 0.27 per day (i.e. approximately each three and a half day). This can be associated with the typical frequency of moving weather systems (extratropical cyclones) (Gulev, Zolina, & Grigoriev, 2001).

The spatial distribution of temperature and humidity is not homogeneous in the barn as shown in Fig. 5. Considering the spatial distribution of temperature on most days we observed colder temperatures at the western side of the barn (sensor 4), which is typically the windward side, compared to the eastern side (e.g., sensor 2). The observed local deviations from the spatial average were up to ±2 °C. Sensor 7, which is close to the short aisle, represented the average barn temperature best, but showed a significantly lower relative humidity than the other three sensors. We observed local deviations in relative humidity up to ±30%. This value was slightly larger than the measurement uncertainty identified in the validation experiment for the Comark devices after long-term exposure to dusty barn air. Thus, despite the large uncertainty in the humidity measurements the deviations can be considered to be significant. While the measurement uncertainty estimated from the validation experiment refers to the instrumentation, the remaining deviation between the measurement locations is attributed to the barn itself.

The observed spatial variations together with the measurement uncertainty resulted in a large range of uncertainty of the estimated THI. This uncertainty is reflected in the estimated values of the different quantiles of the THI distribution calculated from the spatially resolved measurements and shown in Fig. 6. The THI uncertainty is of particular interest during periods where the microclimatic conditions were close to a critical threshold associated with heat stress. According to literature this is the case if THI reached or exceeded a value of 72 (Armstrong, 1994). Considering all events in our time series where the maximal THI was equal or

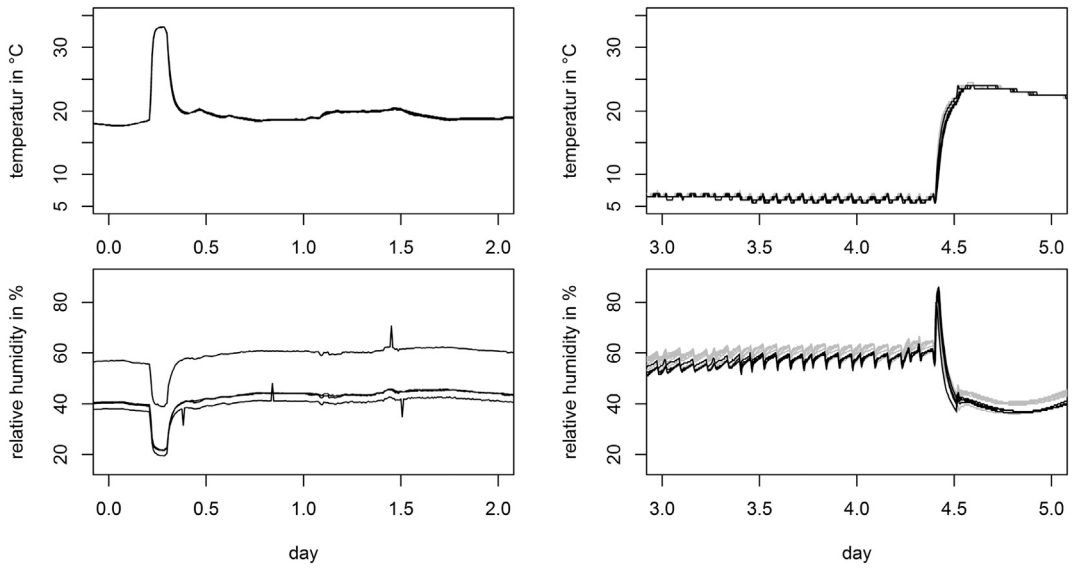

Fig. 3 – Lab experiment with 4 Comark Diligence EV N2003 (left) and 12 EasyLog USB 2+ (right) temperature and humidity sensors. The sensors have been exposed to barn climate over various periods of time before the validation experiment started – for more than 1 year for Comark, about 0.75 years for 8 EasyLog (grey) and about 1 month for 4 EasyLog (black) sensors. First, all Comark devices stayed in an incubator for approximately 2 days (day 0–2). Next, the EasyLog devices were placed in a cold storage cell (day 3–5).

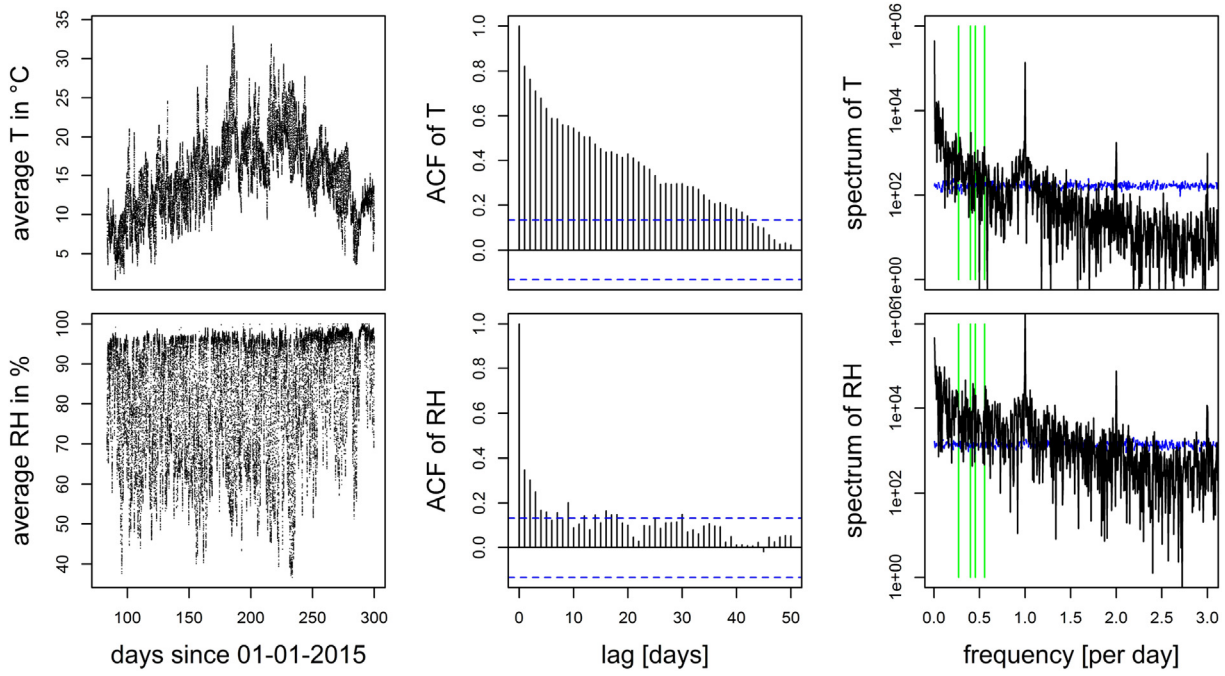

Fig. 4 – Spatially averaged temperature (top) and relative humidity (bottom) data measured inside the barn in Dummerstorf about 3 m above the floor. The left subfigures shows the time series with 10 min resolution measured from spring until autumn 2015. The subfigures in the middle show the corresponding autocorrelation functions for the daily values indicating for how many days the microclimatic conditions are correlated. The dotted line (blue) indicates the confidence interval in the plot. The right subfigures show the periodogram of the considered time series (black) and a reference spectrum of Gaussian white noise with same mean and standard deviation (blue). The vertical lines (green) highlight selected dominant frequencies. (For interpretation of the references to colour in this figure legend, the reader is referred to the web version of this article.)

Table 1 – Seasonal average of ambient daily air temperature (T) and relative air humidity (RH) at the four reference weather stations.

Reference station	Variable	Winter	Spring	Summer	Autumn
Rostock-Warnemünde	T	1.36 °C	7.39 °C	16.69 °C	9.89 °C
Gross Lüsewitz	T	0.67 °C	7.39 °C	16.31 °C	8.86 °C
Brandenburg-Görden	T	0.63 °C	8.33 °C	17.48 °C	9.07 °C
Potsdam	T	0.37 °C	8.72 °C	17.70 °C	9.23 °C
Rostock-Warnemünde	RH	86.70%	78.99%	77.42%	83.23%
Gross Lüsewitz	RH	88.09%	78.04%	77.17%	86.24%
Brandenburg-Görden	RH	84.77%	72.66%	71.62%	82.65%
Potsdam	RH	86.73%	71.59%	71.43%	83.93%

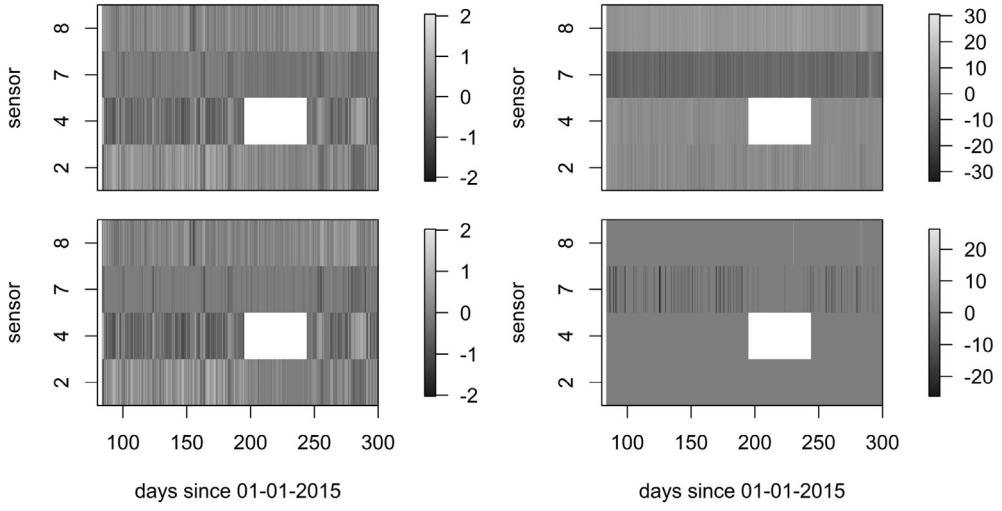

Fig. 5 – Horizontal profile of temperature in °C (left) and relative humidity in % (right) in Dummerstorf. Deviations from the spatial average at each time step are shown. Positive (negative) values indicate local measurements larger (smaller) than the spatial average. The upper row refers to the actual measurement values, while the lower row includes the estimated uncertainty. White areas indicate missing values.

larger than 72 we found that in 83% of the cases the corresponding minimal THI was significantly smaller than 72 (down to 64). On the other hand, 3% of all events denoted as not critical according to the minimal THI correspond to maximal THI larger than 72. These values even go up to 88, which is already classified as emergency. This indicates that the classification of the microclimatic condition into "comfort zone" and "mild stress" and even to "danger" and "emergency" strongly depends on the selected reference point and the associated total measurement uncertainty.

Most critical events lasted only for up to 1 h. There were, however, also several periods where the THI was above 72 for more than 8 h. The cumulated sum for the quantile 0.25 indicated that all events were only included if durations up to 17 h were taken into account. Considering the quantile 0 (minimal THI) this was already the case for durations up to 9 h.

Moreover, we observed that the probability of observing THI values above the critical value of 72 was largest in July where approximately every tenth measurement can be expected to indicate a heat stress condition (cf. Table 2). This means measuring randomly at any time point in July there is a probability of almost 10% to meet a heat stress event. Moreover, there was a not negligible probability to observe critical climatic conditions already in June, while in September nearly no more heat stress events occurred. Comparing different times of the day, the probability to monitor heat stress conditions is largest from noon until evening (i.e., 10 am to 10 pm) where approximately 3% of the data between late March and late November indicated heat stress conditions (cf. Table 2). Considering only the critical conditions we observed that in July, for example, 11% of all events occurred in the night, 8.2% in the morning, 39.7% around noon and 41% in the evening.

3.3. *On-farm experiment barn "Gross Kreutz"*

Similar to the first experiment in Dummerstorf, the time series of the spatially averaged temperature in the barn in Gross Kreutz reflected the annual cycle of the ambient conditions with indoor values up to 39 °C in summer. In spring and autumn indoor temperature went down to 1 °C and in winter down to −8 °C as show in Fig. 7. The observed distribution of temperature values during the year was almost symmetric with a mean of 12.5 °C and a median of 11.6 °C.

The distribution of the measured values of relative humidity on the other hand was asymmetric. With a mean of 74.4% and a median of 78.7% it was significantly drier than in

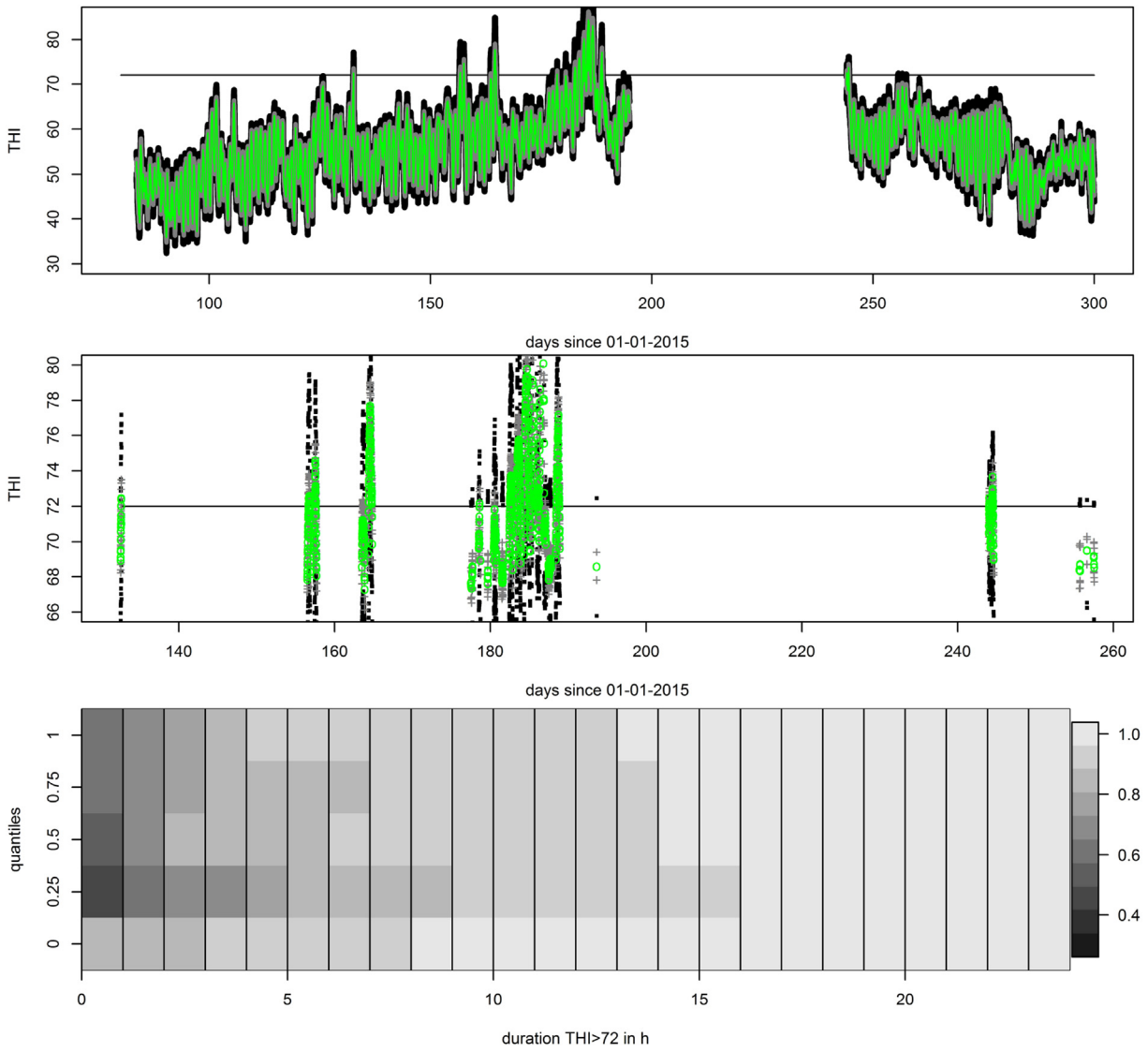

Fig. 6 – Uncertainty in the estimated temperature humidity index (THI) resulting from spatial deviations in temperature and relative humidity and from the estimated measurement device uncertainty for the long-term measurements in Dummerstorf. The upper panel shows the whole THI time series (minimum/maximum in black, 0.25 quantile/0.75 quantile in grey and average in green). The panel in the middle is a zoom into periods around the critical value 72. The lower panel shows the distribution of the duration of events of critical THI (i.e., ≥72) for the different quantiles as normalised cumulative sums. (For interpretation of the references to colour in this figure legend, the reader is referred to the web version of this article.)

Table 2 – Frequency of critical THI values (THI > 72) in % for selected time frames and the two locations Dummerstorf (DT) and Gross Kreutz (GK). The individual months from June until October as well as different times of the day were considered as time frames. The times of the day were defined as follows: night from 10 pm to 4 am (NGT), morning from 4 am to 10 am (MRNG), noon from 10 am to 4 pm (NOON) and evening from 4 pm to 10 pm (EVE).

	Jun	Jul	Aug	Sep	Oct	NGT	MRNG	NOON	EVE
DT	2.3	9.8	NaN	0.6	0.0	0.7	0.5	3.3	2.7
GK	10.6	25.2	36.9	0.8	0.0	1.5	1.3	14.5	12.2

the barn in Dummerstorf. None of the values was above 95% relative humidity (the largest monitored value was 93%). Only one fifth of the values were above 85% relative humidity and two third were above 70% relative humidity, but half of all values were below 75% relative humidity. The lowest values were measured in spring and summer with minima between 26.6% and 32.1% relative humidity which is in accordance with the seasonal averages for the ambient climate (cf. Table 1).

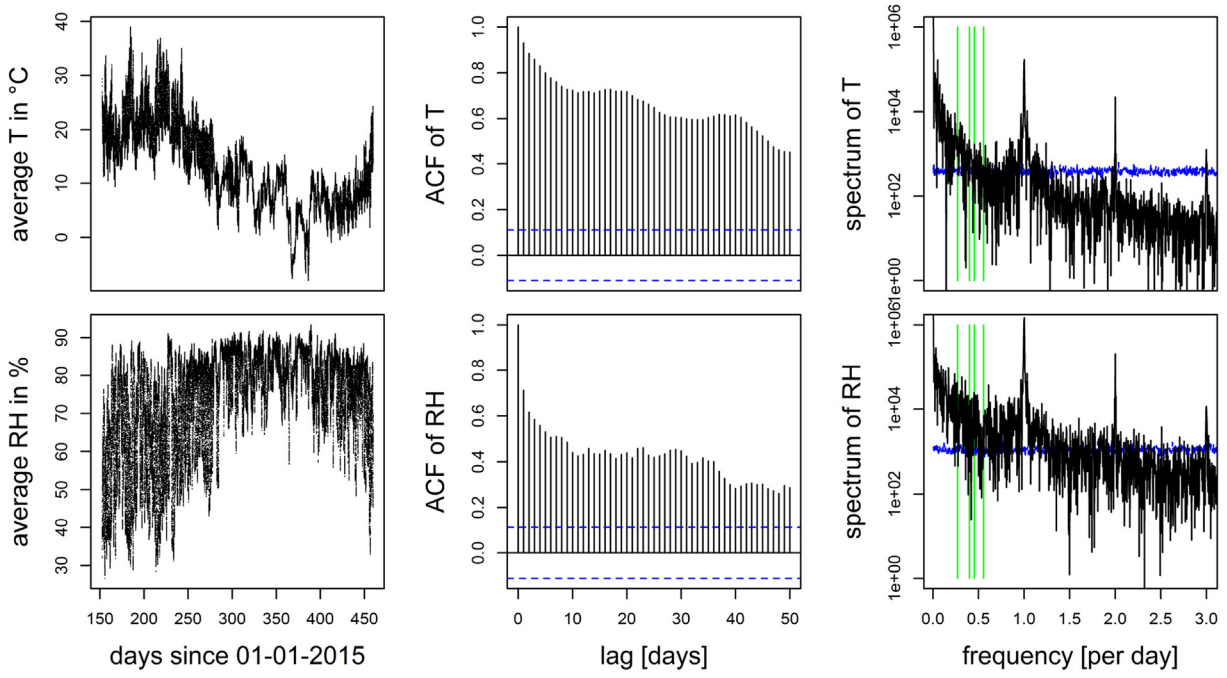

Fig. 7 – Spatially averaged temperature (top) and relative humidity (bottom) data measured inside the barn in Gross Kreutz about 3 m above the floor. The left subfigures shows the time series with 5 min resolution measured from summer 2015 until spring 2016. The subfigures in the middle show the corresponding autocorrelation functions for the daily values indicating for how long the observed microclimatic conditions are correlated. The dotted line (blue) indicates the confidence interval in the plot. The right subfigures show the periodogram of the considered time series (black) and a reference spectrum of Gaussian white noise with same mean and standard deviation (blue). The vertical lines (green) highlight selected dominant frequencies. (For interpretation of the references to colour in this figure legend, the reader is referred to the web version of this article.)

The autocorrelation function decreased much slower than in the first on-farm experiment in Dummerstorf indicating a much higher persistence of the microclimatic conditions. Even after 50 days there was still a significant correlation between the signals, both for temperature ($\geq$0.5) and relative humidity ($\geq$0.3).

Similar to the measurements in Dummerstorf, we found a strong peak at a frequency of 1 per day in the periodogram and smaller peaks at 2 per day and 3 per day where the peak at 2 per day was even more pronounced in Gross Kreutz than in Dummerstorf (cf. Figs. 4 and 5). This shift in the intensity from the peak 3 per day to 2 per day could relate to the different management concepts of the two barns – the barn in Dummerstorf is characterised by milking in groups thrice a day while the barn in Gross Kreutz has an automated milking system. On the weekly time scale, there was again indication for cycles of about 2 days (0.45 per day and 0.55 per day) and 2.5 days (0.4 per day) highlighted by the vertical lines in Fig. 5. However, there are also peaks corresponding to cycles of about 1.5 days and 3 days (0.66 per day and 0.33 per day). The peak around 0.27 per day (i.e. approximately each three and a half day) was less pronounced than in the barn in Dummerstorf, but there was another peak 0.24 per day (approximately a four days cycle) which could be also associated with the transition of extratropical cyclones (Gulev et al., 2001).

Considering the spatial distribution of temperature and relative humidity in the barn in Fig. 8 we observed colder temperature values with the sensors at location R and Z and during some periods at location G and E. Significantly warmer temperatures than the spatial average were particularly observed at location J, O and U which are in the middle of the barn. In some cases, temperatures were up to 4 °C higher than the spatial average at individual locations. For relative humidity we typically monitored significantly dryer situations than the spatial average at the location U, while locations E and J were particularly wet.

Although the measurement uncertainty of the used ensemble of devices was smaller than in the first experiment in Dummerstorf, the distribution of temperature and humidity in the barn in Gross Kreutz let to a significant uncertainty of the estimated THI (cf. Fig. 9). Considering critical events with a maximal THI larger than 72, we found that in 52% of the cases the associated minimal THI was smaller than 72 (down to 64). Thus, these situations would not have been classified as critical according to the minimal THI. On the other hand, 6% of all events denoted as subcritical according to the minimal THI corresponded to maximal THI values considerably larger than 72 (up to 79, i.e. “mild stress” or “danger”). This means that there were situations which were not classified as critical according to a selected individual reference point although there was a significant heat stress risk.

Similar to the results in Dummerstorf, we found that in Gross Kreutz most of the critical events lasted not longer than 1 h. But there were also several periods where the THI was

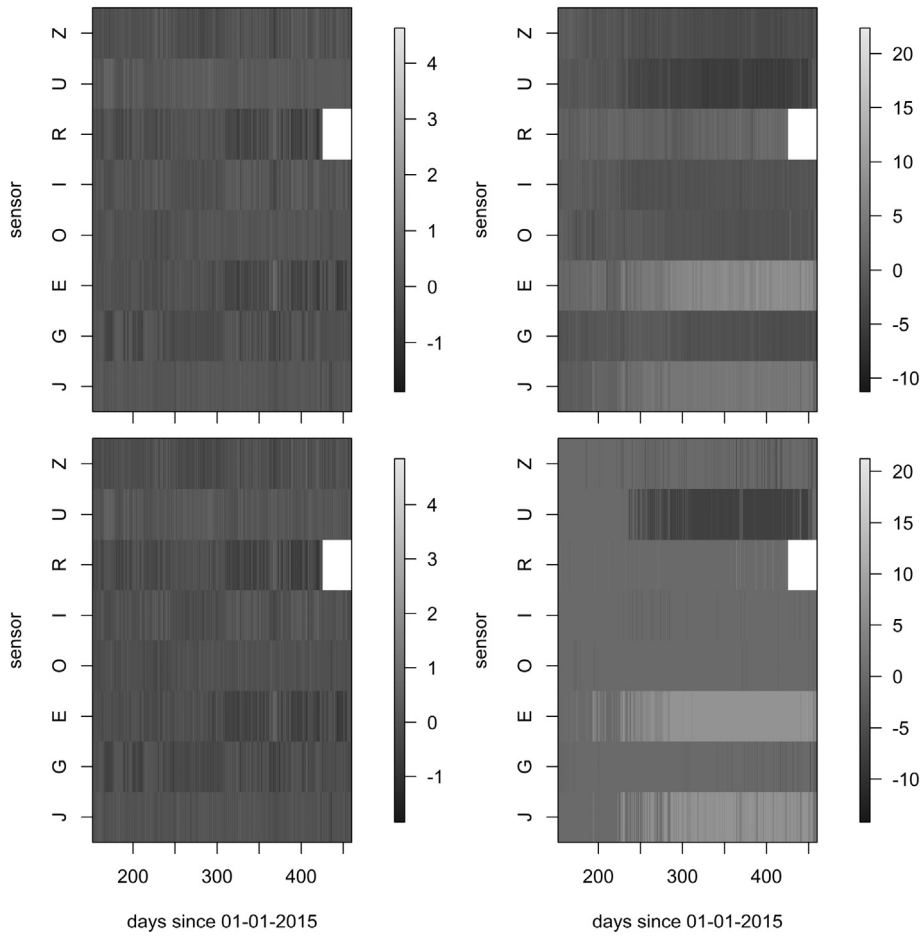

Fig. 8 – Horizontal profile of temperature in °C and relative humidity in % in Gross Kreutz. The deviation from spatial average in each time step for temperature (left) and relative humidity (right) are shown. Positive (negative) values indicate individual measurements larger (smaller) than the spatial average. The upper panels show the actual measurement values, the lower include the estimated uncertainty.

above 72 for more than 8 h. The cumulated sum indicated, for example for the quantile 1 (maximal THI), that all events were only included if durations up to 17 h are taken into account. Considering the quantile 0 (minimal THI) this was already the case for durations up to 14 h. The frequency of longer lasting heat stress conditions was larger in the measurements in Gross Kreutz than in Dummerstorf.

The probability of monitoring heat stress conditions was largest in July and August. In this time frame about 30% of the values were classified as critical. This was the same period as in the measurements in Dummerstorf, but the probability of critical values was nearly three times as large in Gross Kreutz as in Dummerstorf. The probability to observe critical climatic conditions was already about 10% in June, while in September it was nearly vanishing. Considering the whole time series the probability of observing critical conditions was largest from noon until evening (i.e., 10 am to 10 pm) were around 13% of all values indicated critical conditions (cf. 3). Considering only the critical situations in July nearly 88% of all heat stress events occurred between 10 am and 10 pm (in Dummerstorf it were approximately 81%). We observed 6.3% of all events in July in the night, 6.1% in the morning, 46.2% around noon and 41.4% in the evening.

The measurements presented so far were conducted in about 3.4 m height above the floor. The microclimatic conditions in the building at that height are expected to be strongly interrelated with the conditions in the animal occupied zone. Comparing these results to measurements at higher levels in Fig. 10, we observed a significant layering for temperature with warmer temperatures close to the roof (temperature gradient was approximately 0.5 °C per 1 m). The relative humidity at the lowest measured level (close to the animal occupied zone) was significantly higher than at the higher levels. Between 4 m and 6 m there was no significant gradient in humidity.

4. Discussion

4.1. *Total measurement uncertainty*

We found a good agreement for temperature between the measurement devices, where the estimated uncertainty in the considered temperature range was even slightly lower than the accuracy defined by the manufacturer as long as temperature transitions were not too fast (estimated uncertainty

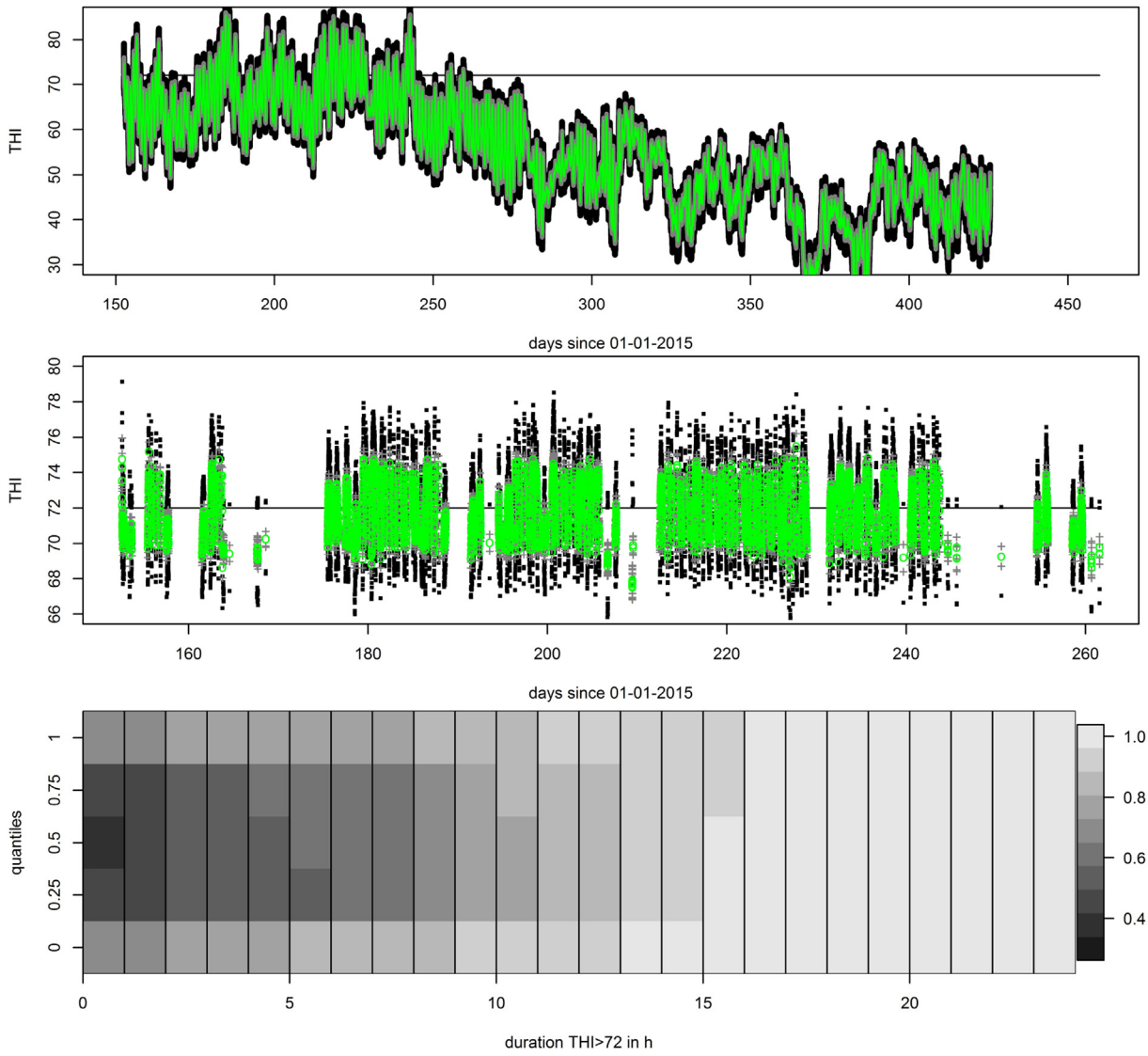

Fig. 9 – Uncertainty in the estimated temperature humidity index (THI) resulting from spatial deviations in temperature and relative humidity and from the estimated measurement device uncertainty for the long-term measurements in Gross Kreutz. The upper panel shows the whole THI time series (minimum/maximum in black, 0.25 quantile/0.75 quantile in grey and average in green). The panel in the middle is a zoom into periods around the critical value 72. The lower panel shows the distribution of the duration of events of critical THI (i.e., ≥72) for the different quantiles as normalised cumulative sums. (For interpretation of the references to colour in this figure legend, the reader is referred to the web version of this article.)

for Comark device 0.4 °C instead of 0.5 °C and for EasyLog 0.6 °C instead of 1 °C). The largest deviations between the simultaneous temperature measurements occurred after fast temperature changes (>10 °C h^{-1}). This increase in uncertainty can be partially attributed to the reaction time of the device. In addition, during these transition periods the assumption of a homogenous temperature distribution inside the test volume might be not fulfilled. Thus, the uncertainty values estimated during the slow temperature changes (<3 °C h^{-1}) can be considered more representative to evaluate the on-farm measurements. Moreover, the slow changes can be considered as more representative for the on-farm measurements as fast temperature drops of 10 °C h^{-1} occur only on rare occasions (e.g. during thunderstorms).

For relative humidity, the observed uncertainty in the validation experiment was much higher than the accuracy defined by the manufacturer. The accuracy, however, refers to the instrumentation uncertainty, which is only a part of the potential total measurement uncertainty. In our experiment, even in a regime with slow transitions in temperature and relative humidity the observed uncertainty in relative humidity was twice as large as the stated accuracy of the devices in case of the EasyLog (7% instead of 3.5%). In case of the Comark devices the uncertainty in relative humidity was with 26% (instead of 3% instrumentation uncertainty according to the manufacturer) even higher.

As shown in the results, there was a considerable uncertainty in relative humidity measurements attributed to

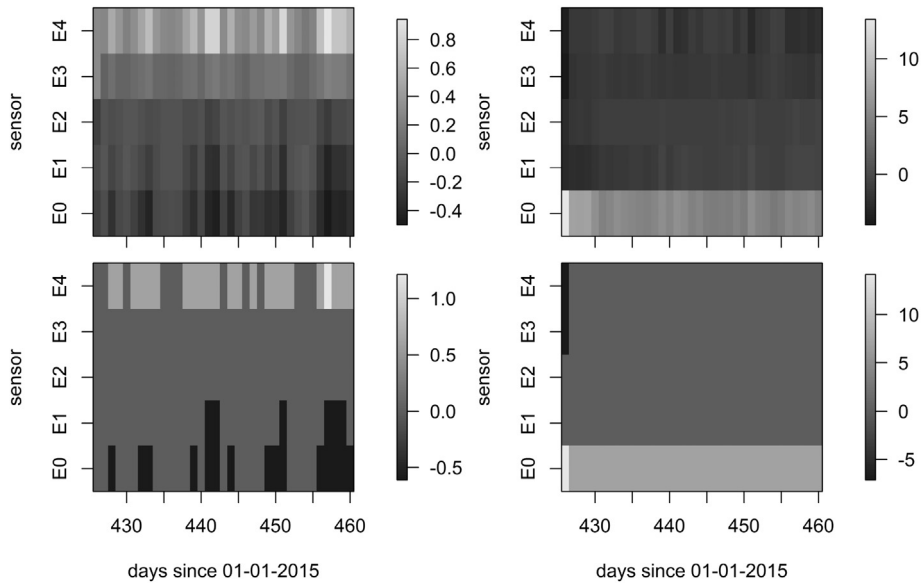

Fig. 10 – Vertical profile of temperature in and relative humidity in % in Gross Kreutz. The deviations from spatial average in each time step for temperature (left) and relative humidity (right) at the sensor location E are shown. Daily average values are presented here. The upper panels show the actual measurement values, the lower panels include the estimated uncertainty.

general aging effects and the measurement history of the ensemble of devices in use. A possible reason for the large deviation between the instrumentation uncertainty and the total measurement uncertainty in the validation experiment might be a contamination of the measurement devices with small particles during the on-farm measurements. This contamination results in a bias for the individual devices. In consequence, the uncertainty for the ensemble of measurement devices increases, since the contamination will not be uniformly for all devices. This assumption is supported by the observation that devices that have been in use for a long time under on-farm conditions tended to show higher relative humidity values in the validation experiment than devices that were exposed to on-farm conditions only for a short period. In consequence, continuous long-term measurements of relative humidity under on-farm conditions have to be attributed with larger uncertainty than short-term measurements with the same device even if the surface of the device is cleaned regularly. By implication, the measurement uncertainty for long-term monitoring of relative humidity under on-farm conditions could be reduced by a sound regular cleaning of the devices.

4.2. *Comparison of the two building sites*

The observed range and distribution of indoor temperatures was similar in both locations. In addition, the indoor temperature time series in both experiments showed a strong persistence. In Dummerstorf we found significant correlations up to a time lag of about 40 days. In Gross Kreutz the persistence time was even a bit longer. These values are much higher than the typical persistence time for atmospheric temperature values documented in literature which is about 5 days (Wilks, 2011). However, compared with the autocorrelation of the signal at the reference weather stations (example year 2000) the decay of the autocorrelation function in Gross Kreutz represents the persistence of the outdoor references (Brandenburg-Görden and Potsdam) quite well (see Table 3). For Dummerstorf, the decay of the autocorrelation function is even faster for the indoor data collected in our experiment than for the two reference stations (Gross Lüsewitz and Rostock-Warnemünde). However, the autocorrelation functions of these two reference stations also differ much more from each other than those for Brandenburg-Görden and Potsdam (see Table 3). This further complicates the definition of a suitable climate reference for impact studies.

Moreover, we observed that the persistence in general was stronger in Gross Kreutz than in Dummerstorf. For a lag of 5 days, for example, the correlation was about 0.8 for the on-farm experiment in Gross Kreutz and 0.6 for the one in Dummerstorf. While in Dummerstorf the autocorrelation was even lower than at the reference stations, in Gross Kreutz it was slightly higher than the value at the corresponding reference stations. This is in accordance with the fact that the barn in Dummerstorf is much more open than the one in Gross Kreutz. In consequence, the temperature in the barn in Dummerstorf is more directly affected by the ambient temperature, while in the barn in Gross Kreutz the temperature input might be more damped by the building material.

Considering the humidity data, we found larger deviations between the two measurement sites, both with regard to the range and the distribution of the relative humidity values. The relative humidity in Gross Kreutz was on average approximately 10% lower than in Dummerstorf. This is probably a result of two effects:

Table 3 – Autocorrelations at three different lags based on one year of daily temperature/relative humidity data (2000) at the four reference weather stations.

Reference station	lag 5	lag 10	lag 40
Gross Lüsewitz	0.76/0.31	0.70/0.29	0.46/0.20
Rostock	0.79/0.21	0.73/0.21	0.48/0.08
Brandenburg	0.75/0.40	0.70/0.40	0.45/0.24
Potsdam	0.76/0.45	0.71/0.46	0.44/0.25

(1) There is a difference in the average humidity of the incoming air flow. Based on the data from the reference weather stations the relative humidity in Dummerstorf can be expected to be approximately 1%–7% larger than in Gross Kreutz (depended on the season and the selected reference station, cf. Table 1).

(2) There is a larger uncertainty attributed to the devices used for the study in Dummerstorf. These devices have been exposed to the dusty barn air much longer in advance of the study. Thus as discussed in the paragraph "total measurement uncertainty", we can expect also a bias in terms of a systematic offset in the Dummerstorf data set, which can explain the remaining deviation in the average relative humidity.

The persistence in the time series of relative humidity was much smaller than for temperature in both experiments. However, in Gross Kreutz correlation coefficients of approximately 0.3 were still obtained for a time lag of 40 days, while the autocorrelation is almost zero in Dummerstorf for the same time lag. These values are comparable to autocorrelation functions at the corresponding reference stations (except for Gross Lüsewitz which is characterised by a much higher persistence in the relative humidity than Rostock and Dummerstorf).

The comparison of the two building sites illustrates that even in one country a generalisation of the microclimatic conditions in naturally ventilated barns is challenging (at least as long as the microclimatic conditions are governed predominantly by the weather and not by automated active management of the ventilation). While the temperature distribution is rather homogeneous and correlates well with the ambient conditions the dynamics in relative humidity may differ significantly between the barns. Thus, detailed spatially resolved measurements or a detailed knowledge of the airflow patterns, the distribution of moisture sources in the barn and the dynamics of the ambient climate are required to obtain good estimates of the relative humidity in naturally ventilated barns. In this context, it must be noted that the geographically nearest station must not necessarily be the most representative for the dynamics of the ambient conditions (cf. data from Gross Lüsewitz and Rostock-Warnemünde).

4.3. *Horizontal temperature and humidity distribution in naturally ventilated barns*

In the long-term experiments in Dummerstorf and Gross Kreutz we observed a rather homogeneous temperature distribution approximately 3 m above the ground. In this height, we typically observe spatial fluctuations in temperature in an order of magnitude of ±2 °C deviation from the spatial average. Spatial fluctuations in the relative humidity are, however, within an order of magnitude of ±20% relative humidity deviation from the spatial average comparably large (cf. Fig. 5). This may be related to the distribution of cows in the barn, which are a main source of humidity. Additional impact factors might be the locations of water troughs or urine puddles.

On the other hand, it also reflects the incomplete mixing of used and fresh air. The air flow through the building is essential for the removal of moisture. However, there are areas with long and short residence times inside a barn (Hempel et al., 2015). Thus, the air flow patterns affect the felt air temperature not only via different air speeds, but notably also by varying the water vapour content of the air.

This is of particular importance during hot periods where the animals seek for evaporative cooling (e.g., by transpiration). Due to the inhomogeneous distribution of relative humidity (and temperature) though out the barn, cows may feel more comfortable in particular areas than in other ones. This fragmentation of the animal occupied zone does, however, not necessarily overlap with the practical partition of the barn into functional areas (e.g., for feeding, drinking or milking). In consequence, during uncomfortable weather situations inhomogeneity in the microclimatic conditions in the animal occupied zone may imply a higher stress level in the herd as the animals will try to gather at less floor space. Hence, a more homogeneous distribution of the microclimatic conditions can decrease the stress level and by that increase animal welfare, health and productivity. Improved ventilation concepts have to take the spatial distribution of temperature, humidity and air speed into consideration in order to avoid undesirable changes in animal behaviour as a reaction to heat stress.

In addition, our results indicate that a single temperature-humidity-sensor inside the barn is not enough to assess the risk of heat stress based on microclimatic parameters. A detailed knowledge of the distribution of wind speed and humidity inside the building for inflow conditions, under which heat stress could occur, is required.

4.4. *Vertical temperature and humidity profile*

Earlier studies indicated that in naturally ventilated barns air flow often results in a jet in the lower levels of the barn and some kind of recirculation in the upper levels (Hempel et al., 2015). Air exchange between these regions is limited.

In our time series, relative humidity was significantly higher in the lowest measured level than in the overlying levels. The observed homogeneous humidity distribution in the upper layers supports the assumption of two widely decoupled air volumes - one in the animal occupied zone and one close to the roof. The degree of mixing within those layers is expected to be significantly higher than between the layers.

Considering the cows as a significant heat source in the animal occupied zone, we expect buoyancy effects resulting from the heating of air subvolumes and facilitating vertical mixing. The wind speed associated with this vertical convection is with an order of magnitude of cm s^{-1} rather slow. Thus for situations with a powerful cross-ventilation, the vertical

wind speed would be much too slow compared with the horizontal flow to trigger significant vertical mixing.

However, in our experiments we monitored many situations where the horizontal wind speed in 3 m height was only approximately twice as large as the vertical wind speed. Thus, in that height the horizontal wind speed was too slow to suppress the vertical mixing. This could indicate that at this height there was no sufficient cross-ventilation.

The two apparently contradictory observations of a not negligible vertical air speed (based on air velocity measurement in 3 m height) and the decoupling of the air volumes below 3.4 m and above 4 m (based on measurements of relative humidity in the two heights) implies that the shear flow in the building under investigation was between 3.4 m and 4 m height. Below this shear flow (i.e., in the animal occupied zone) horizontal wind speed was sufficiently low to permit vertical mixing.

Across both zones, heat radiation from the animals contributes to the heat interchange between the roof and the indoor air.

A better understanding of the spatial and temporal distribution of the air velocity is required to quantify the actual air flow patterns, the resulting transport of humidity, the mixing properties and the separation of air volumes in detail.

The observed deviations in relative humidity (upto 15% relative humidity, cf. Fig. 10) between the layers can be attributed to three effects:

(1) Even with a constant water vapour content the relative humidity decreases towards the roof as the temperature increases. Assuming an average temperature of 1 °C and average humidity of 50% in the barn at 3.4 m as typical conditions for early March, the expected decrease of relative humidity purely caused by the observed temperature increase was estimated to be approximately 5%. Thus, on average approximately one third of the difference of relative humidity between the upper and the lower air volume in our data set would be explained by the increased storage capacity of water vapour in the warmer air. This value can be even higher for particular combinations of temperature and relative humidity.
(2) There is a considerable entry of additional water vapour from the cows in the lower air volume. For the temperature range considered (0 °C upto 25 °C) a cow is expected to produce approximately 0.5 g–1 g water vapour per second (DIN, 2004; Pedersen & Sällvik, 2002). Approximating the lower air volume in the barn with 1350 m^3, 45 cows are expected to add on average approximately 0.5*45/1350 g = 0.0167 g to 1*45/1350 g = 0.0334 g water vapour per second to a subvolume of 1 m^3 of air. Assuming a cross-ventilation with approximately 0.5 m s^{-1} average wind speed in the animal occupied zone, such a subvolume of air would need about 1 min to cross the whole barn (approximately 30 m). In this minute, a total of 1 g up to 2 g water per m^3 is added. At 25 °C, this corresponds to approximately 3 or 7% relative humidity. At 0 °C, this corresponds to approximately 20 or 41% relative humidity. Hence, this can explain one third up to all of the difference of relative humidity between the upper and the lower air volume in our data set depending on the actual temperature.
(3) Other potential sources of additional water vapour in the animal occupied zone are water troughs, slurry and urine puddles.

The sensors could not be positioned lower in this study, because devices to protect the sensors from the animals were not available. Since air speed in the lower volume is sufficiently low to permit vertical mixing, the measurements of relative humidity (including the horizontal variability) in about 3.4 m height were assumed to be at least functionally related to the conditions at the lower edge of the jet, which corresponds for most of the floor area to the emission-active zone. Whether this measuring height or a lower one is representative for the floor area, further studies with measurements in the AOZ will have to show.

In the case of temperature, we observed in the upper air volume a small temperature gradient with higher values at the roof and lower values towards the middle of the barn. This can be interpreted as a result of radiative heat fluxes (caused by sunshine and animal heat radiation) combined with a limited air exchange of the upper air volume and the upwelling of warm air. We expect higher gradients in the animal occupied zone, with largest values close to the animal bodies. However, to verify this assumption, further measurements of vertical profiles are needed which cover heights from the floor up to the roof and need to be conducted with devices with a higher accuracy in the temperature measurement.

4.5. *Temperature-humidity-index*

In literature, the decline rate of milk production per THI unit in subtropical climate was estimated to range from −0.30 kg to −0.39 kg per cow and day, dependent on whether the cows are living in a humid or a semiarid climate (Bohmanova et al., 2007). Other authors highlighted that Holstein populations in Europe producing in temperature climates showed heat stress (in terms of a decrease in milk quality and yield) at lower heat loads than those cattle producing in warmer climate (Carabano et al., 2016). Moreover, these authors showed that the milk quality (fat and protein content) is affected even at lower THI values than milk yield. In an other study, it was shown that under heat stress conditions in mediterranean climate a temperature increase of 1 °C (with constant relative humidity, according to Eq. (3) this corresponds to an increase in THI units by approximately 1–2) is associated with on average approximately 1 kg decrease in milk yield and 1.5 l increase in water consumption per cow and day (Bouraoui et al., 2002).

Considering the differences between the minimal and maximal estimated THI value for each time step, we obtain uncertainty values for the THI (i.e., in terms of twice the standard deviation of the observed differences) of approximately ±4 in the measurements in Dummerstorf and ±2 in the measurements in Gross Kreutz. This corresponds to 1.2 kg up to 8 kg difference per day in the approximated milk yield loss per cow and day for Dummerstorf and 0.6 kg up to 4 kg per cow and day for Gross Kreutz. The difference in the estimated rise

in water intake per cow is up to 12 l for Dummerstorf and up to 6 l for Gross Kreutz. In consequence, the uncertainty in temperature and particularly relative humidity measurements results in an uncertainty in the heat stress assessment which relates to a significant uncertainty in welfare and economic impact assessment. This uncertainty must be added to uncertainty in the THI threshold that results from the different adaptability of individual cows in various climate zones.

5. Conclusion

Our study showed that the uncertainty attributed to measurements of the microclimatic conditions in naturally ventilated dairy barns is notably determined by the accuracy of the humidity monitoring. This uncertainty is propagated to animal welfare assessment based on the classical temperature humidity index.

For temperature, the uncertainty was mainly determined by the instrumentation uncertainty (≈ ±0.5 °C) and the spatial variability (≈ ±2 °C).

For relative humidity, the uncertainty sources were considerably larger. While the instrumentation uncertainty was approximately ±4% relative humidity, the observed spatial deviations were up to approximately ±20%. The later value depends on the inflow conditions and the building design. In addition, we found a bias in relative humidity measurements related to the age and the measurement history of the devices. Devices that have been in use for a long time under on-farm conditions tend to show larger relative humidity values (≈ +4% in our validation experiment) due to contamination. Since the contamination of the devices in a barn is usually not homogenous, this results in an ensemble uncertainty for the spatially resolved measurements (≈ ±2%). In consequence, the total measurement uncertainty for relative humidity should be assessed for each building and measurement campaign individually.

Furthermore, our results indicated that a single temperature humidity sensor inside the barn is not enough to assess the risk of heat stress based on microclimatic parameters. Even if the instrumentation uncertainty and the ensemble uncertainty are known, without a detailed knowledge of the distribution of air velocity and humidity in the building the estimated temperature humidity index (THI) is a very uncertain measure for heat stress risk.

The inhomogeneous distribution of relative humidity throughout the barn results in different comfort zones that do not necessarily overlap with the functional zones in the barn. This is of particular importance during hot periods, as increasingly expected under climate change, where the animals seek for evaporative cooling (e.g., by transpiration). Representative sensor positions and smart ventilation concepts that take the spatial distribution of humidity into consideration are required to avoid undesirable changes in animal behaviour as a reaction to heat stress.

In our study we measured the microclimatic conditions in the animal occupied zone indirectly in a height of about 3 m–3.5 m. The measured flow regimes in the barn suggest that this height could represent the conditions in the animal occupied zone. However, investigations of the most representative sensor positions along this cross-section have to be conducted for each barn individually to reduce the uncertainty in animal welfare assessment in terms of THI. It will potentially be possible to derive general recommendations for the horizontal and vertical distribution of the sensors when more data become available (e.g., spatially resolved long-term measurements in a large number of barns and measurements in the animal occupied zone with suitable devices).

Moreover, risk assessment as well as adaptation concepts in terms of smart ventilation must consider also the uncertainty attributed to the individual physiological and behavioural response of the cows to the actual microclimatic conditions.

Acknowledgements

This study was conducted in the framework of the OptiBarn project in the FACCE ERANET+ initiative on climate smart agriculture.

The work was financially supported by the German Federal Ministry of Food and Agriculture (BMEL) through the Federal Office for Agriculture and Food (BLE), grant number 2814ERA02C.

We thank Klaus Parr and Detlef May for permitting to conduct the long-term measurements at their farms.

We further thank Knut Schröter, Ulrich Stollberg, Andreas Reinhardt and Detlef Werner, technicians at ATB, for supporting the implementation of the measurements.

REFERENCES

Algers, B., Bertoni, G., Broom, D., Hartung, J., Lidfors, L., Metz, J., et al. (2009). Effects of farming systems on dairy cow welfare and disease. Scientific report of EFSA prepared by the Animal Health and Animal Welfare Unit on the effects of farming systems on dairy cow welfare and disease *Annex to the EFSA Journal, 1143*, 1–38.

Armstrong, D. (1994). Heat stress interaction with shade and cooling. *Journal of Dairy Science, 77*, 2044–2050.

Banhazi, T. (2013). Seasonal, diurnal and spatial variations of environmental variables in Australian livestock buildings. *Australian Journal of Multi-disciplinary Engineering, 10*, 60–69.

Bjerg, B., Norton, T., Banhazi, T., Zhang, G., Bartzanas, T., Liberati, P., et al. (2013). Modelling of ammonia emissions from naturally ventilated livestock buildings. Part 1: Ammonia release modelling. *Biosystems Engineering, 116*, 232–245.

Bohmanova, J., Misztal, I., & Cole, J. (2007). Temperature-humidity indices as indicators of milk production losses due to heat stress. *Journal of Dairy Science, 90*, 1947–1956.

Bouraoui, R., Lahmar, M., Majdoub, A., Djemali, M., & Belyea, R. (2002). The relationship of temperature-humidity index with milk production of dairy cows in a mediterranean climate. *Animal Research, 51*, 479–491.

Carabano, M.-J., Logar, B., Bormann, J., Minet, J., Vanrobays, M.-L., Díaz, C., et al. (2016). Modeling heat stress under different environmental conditions. *Journal of Dairy Science, 99*, 3798–3814.

Chan, K.-S., & Ripley, B. (2012). *TSA: Time series analysis*. http://CRAN.R-project.org/package=TSA r package version 1.01.

Christensen, J., Hewitson, B., Busuioc, A., Chen, A., Gao, X., Held, I., et al. (2007). Regional climate projections. In *IPCC climate change 2007: The physical science basis*.

DIN. (2004). *Thermal insulation for closed livestock buildings – Thermal insulation and ventilation forced. Part 1: Principles for planning and design for closed ventilated livestock buildings*. German Institute for Standardization (DIN).

Gulev, S., Zolina, O., & Grigoriev, S. (2001). Extratropical cyclone variability in the northern hemisphere winter from the NCEP/NCAR reanalysis data. *Climate Dynamics, 17*, 795–809.

Hempel, S., Saha, C. K., Fiedler, M., Berg, W., Hansen, C., Amon, B., et al. (2016). Non-linear temperature dependency of ammonia and methane emissions from a naturally ventilated dairy barn. *Biosystems Engineering, 145*, 10–21.

Hempel, S., Wiedemann, L., Ammon, C., Fiedler, M., Saha, C., Loebsin, C., et al. (2015). Assessment of the through-flow patterns in naturally ventilated dairy barns – three methods, one complex approach. In I. Körner (Ed.), *RAMIRAN 2015 rural-urban symbiosis TC-O_16* (pp. 356–359). Germany: TUTech Verlag, Hamburg, Germany: Hamburg University of Technology. E-book.

Kendall, P., Nielsen, P., Webster, J., Verkerk, G., Littlejohn, R., & Matthews, L. (2006). The effects of providing shade to lactating dairy cows in a temperate climate. *Livestock Science, 103*, 148–157.

Kuczynski, T., Blanes-Vidal, V., Li, B., Gates, R. S., Alencar Naas, I. d., Moura, D. J., et al. (2011). Impact of global climate change on the health, welfare and productivity of intensively housed livestock. *International Journal of Agricultural and Biological Engineering, 4*, 1–22.

Mader, T. L., Davis, M., & Brown-Brandl, T. (2006). Environmental factors influencing heat stress in feedlot cattle. *Journal of Animal Science, 84*, 712–719.

Monteny, G.-J., Bannink, A., & Chadwick, D. (2006). Greenhouse gas abatement strategies for animal husbandry. *Agriculture, Ecosystems & Environment, 112*, 163–170.

National Research Council. (1971). *A guide to environmental research on animals*. Washington, DC: National Academy of Science.

Pedersen, S., & Sällvik, K. (2002). *Climatization of animal houses-heat and moisture production at animal and house level 4th report of CIGR working group*. Horsens, Demark: Research Centre Bygholm, Danish Insitute of Agricultural Sciences.

R Core Team. (2015). *R: A language and environment for statistical computing*. Vienna, Austria: R Foundation for Statistical Computing. http://www.R-project.org/.

Ravagnolo, O., Misztal, I., & Hoogenboom, G. (2000). Genetic component of heat stress in dairy cattle, development of heat index function. *Journal of Dairy Science, 83*, 2120–2125.

Rong, L., Liu, D., Pedersen, E. F., & Zhang, G. (2014). Effect of climate parameters on air exchange rate and ammonia and methane emissions from a hybrid ventilated dairy cow building. *Energy and Buildings, 82*, 632–643.

Saha, C., Ammon, C., Berg, W., Fiedler, M., Loebsin, C., Sanftleben, P., et al. (2014). Seasonal and diel variations of ammonia and methane emissions from a naturally ventilated dairy building and the associated factors influencing emissions. *Science of the Total Environment, 468*, 53–62.

Schrade, S., Zeyer, K., Gygax, L., Emmenegger, L., Hartung, E., & Keck, M. (2012). Ammonia emissions and emission factors of naturally ventilated dairy housing with solid floors and an outdoor exercise area in Switzerland. *Atmospheric Environment, 47*, 183–194.

Venables, W. N., & Ripley, B. D. (2013). *Modern applied statistics with S-PLUS*. Springer Science & Business Media.

Vlachos, M., Philip, S. Y., & Castelli, V. (2005). On periodicity detection and structural periodic similarity. In *SDM* (Vol. 5, pp. 449–460). SIAM.

Wilks, D. S. (2011). *Statistical methods in the atmospheric sciences* (Vol. 100). Academic press.